

Supplementary material

[1SM] Castelo Bandane Vilanculo, Márcio José da Silva, Sukarno Olavo Ferreira, Milena Galdino Teixeira, *A rare oxidation of camphene to acid and aldehyde in the presence of Lacunar Keggin heteropoly salts*, *Molecular Catalysis* 478 (2019) 110589-110595

Received 23 July 2019; Received in revised form 19 August 2019; Accepted 23 August 2019.

List of Figures

Figure SM1. FT-IR spectra of phosphomolybdic acid and its lacunar sodium salt

Figure SM2. FT-IR spectra of silicotungstic acid and its lacunar sodium salt

Figure SM3. Powdered XRD patterns of $\text{Na}_7\text{PMo}_{11}\text{O}_{39}$ lacunar salt and parent $\text{H}_3\text{PMo}_{12}\text{O}_{40}$

Figure SM4. Powdered XRD patterns of $\text{Na}_8\text{SiW}_{11}\text{O}_{39}$ lacunar salt and parent $\text{H}_4\text{SiW}_{12}\text{O}_{40}$

Figure SM5. TG/DSC curves: precursor $\text{H}_3\text{PMo}_{12}\text{O}_{40}$ (a) and $\text{Na}_7\text{PMo}_{11}\text{O}_{39}$ lacunar salt (b)

Figure SM6. TG/DSC curves: $\text{H}_4\text{SiW}_{12}\text{O}_{40}$ precursor (a) and $\text{Na}_8\text{SiW}_{11}\text{O}_{39}$ lacunar salt (b)

Figure SM7. Potentiometric titration curves with *n*-butylamine of $\text{H}_3\text{PMo}_{12}\text{O}_{40}$ and $\text{Na}_7\text{PMo}_{11}\text{O}_{39}$ salt

Figure SM8. Potentiometric titration curves with *n*-butylamine of $\text{H}_4\text{SiW}_{12}\text{O}_{40}$ and $\text{Na}_8\text{SiW}_{11}\text{O}_{39}$ salt

Figure SM9: Scanning electronic microscopy images of sodium salts; $\text{Na}_3\text{PW}_{12}\text{O}_{40}$, $\text{Na}_7\text{PMo}_{11}\text{O}_{39}$ and $\text{Na}_8\text{SiW}_{11}\text{O}_{39}$

Figure SM10: EDS data of $\text{Na}_3\text{PW}_{12}\text{O}_{40}$, $\text{Na}_7\text{PMo}_{11}\text{O}_{39}$ and $\text{Na}_8\text{SiW}_{11}\text{O}_{39}$

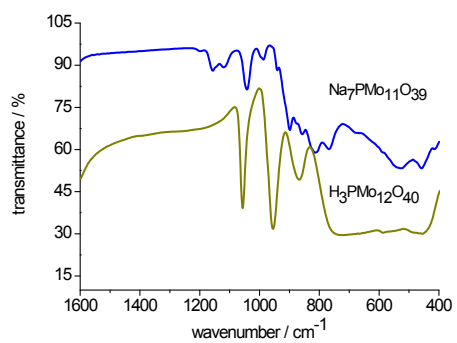


Figure SM1. FT-IR spectra of phosphomolybdic acid and its lacunar sodium salt

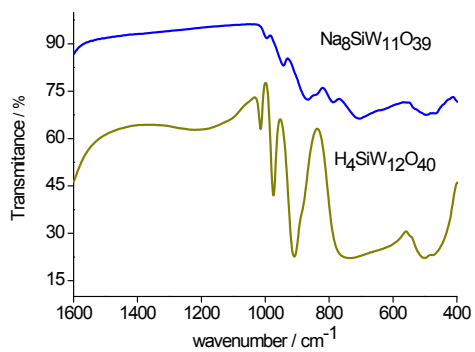


Figure SM2. FT-IR spectra of silicotungstic acid and its lacunar sodium salt

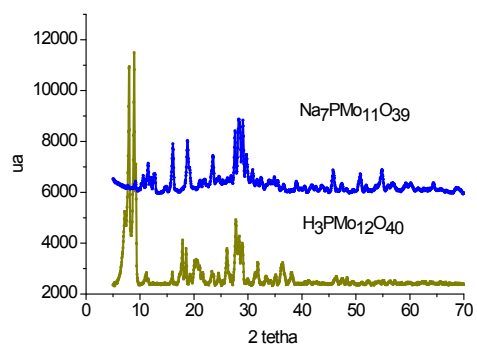


Figure SM3. Powdered XRD patterns of Na₇PMo₁₁O₃₉ lacunar salt and parent H₃PMo₁₂O₄₀

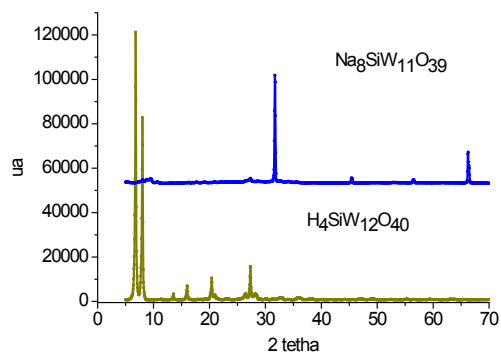


Figure SM4. Powdered XRD patterns of $\text{Na}_8\text{SiW}_{11}\text{O}_{39}$ lacunar salt and parent $\text{H}_4\text{SiW}_{12}\text{O}_{40}$

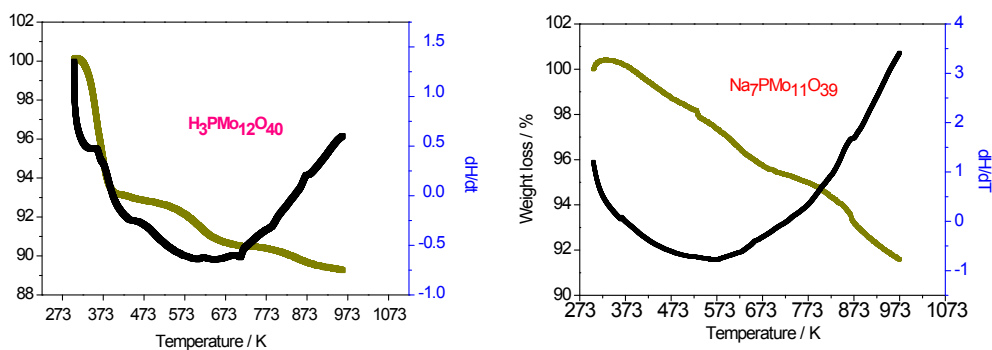


Figure SM5. TG/DSC curves: precursor $\text{H}_3\text{PMo}_{12}\text{O}_{40}$ (a) and $\text{Na}_7\text{PMo}_{11}\text{O}_{39}$ lacunar salt (b)

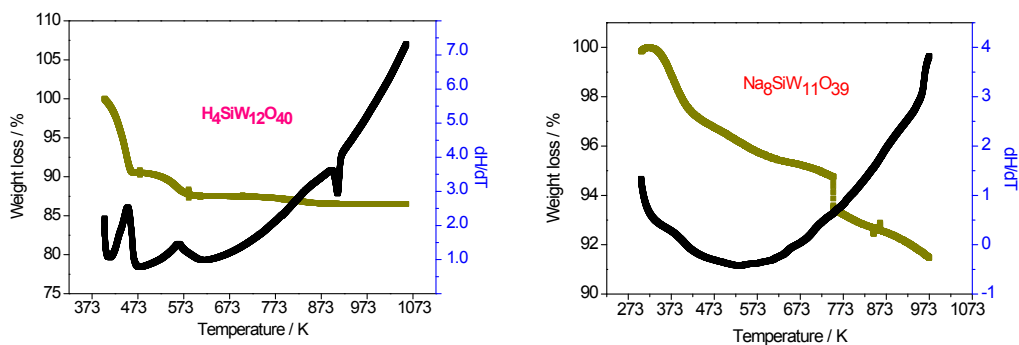


Figure SM6. TG/DSC curves: precursor $\text{H}_4\text{SiW}_{12}\text{O}_{40}$ (a) and $\text{Na}_8\text{SiW}_{11}\text{O}_{39}$ lacunar salt (b)

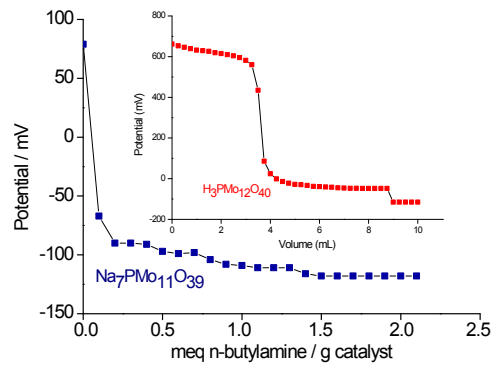


Figure SM7. Potentiometric titration curves with *n*-butylamine of $\text{H}_3\text{PMo}_{12}\text{O}_{40}$ and $\text{Na}_7\text{PMo}_{11}\text{O}_{39}$ salt

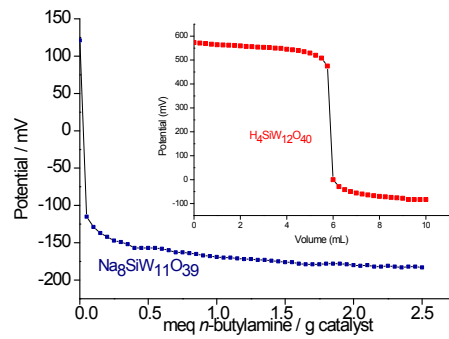


Figure SM8. Potentiometric titration curves with *n*-butylamine of $\text{H}_4\text{SiW}_{12}\text{O}_{40}$ and $\text{Na}_8\text{SiW}_{11}\text{O}_{39}$ salt

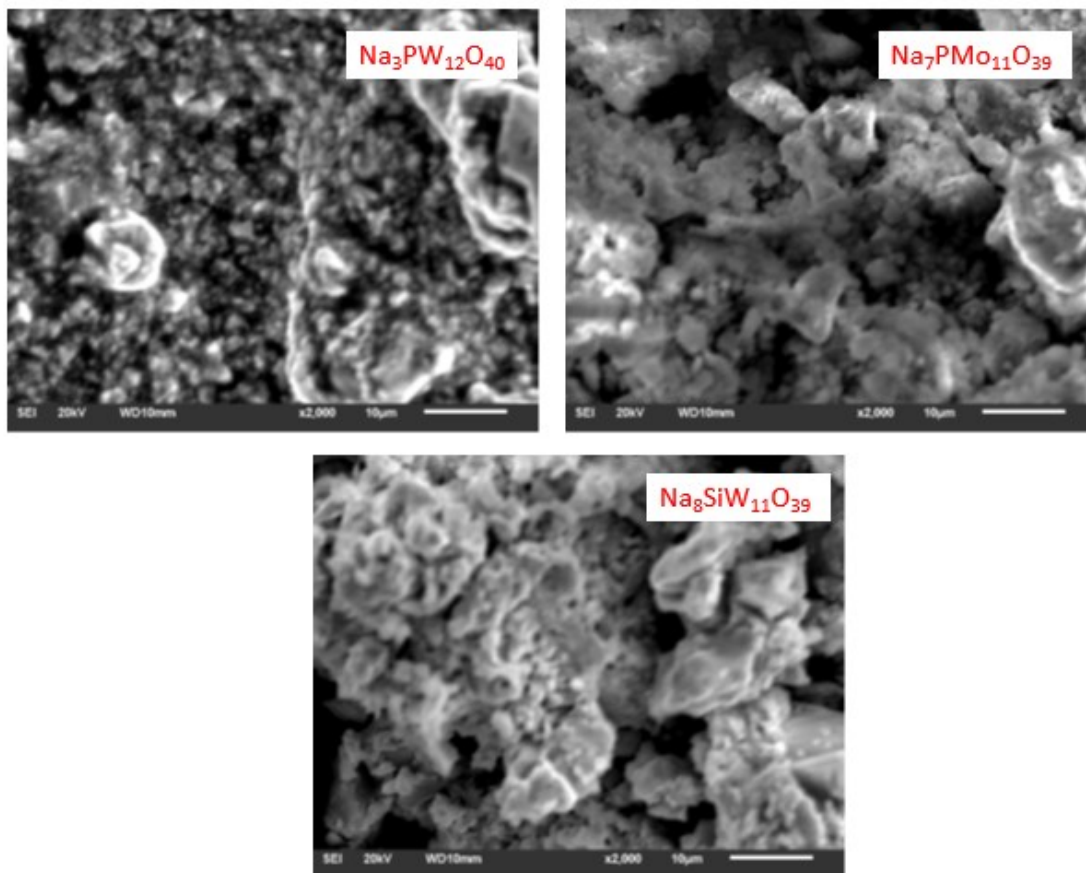


Figure SM9: Scanning electronic microscopy images of sodium salts; $\text{Na}_3\text{PW}_{12}\text{O}_{40}$, $\text{Na}_7\text{PMo}_{11}\text{O}_{39}$ and $\text{Na}_8\text{SiW}_{11}\text{O}_{39}$

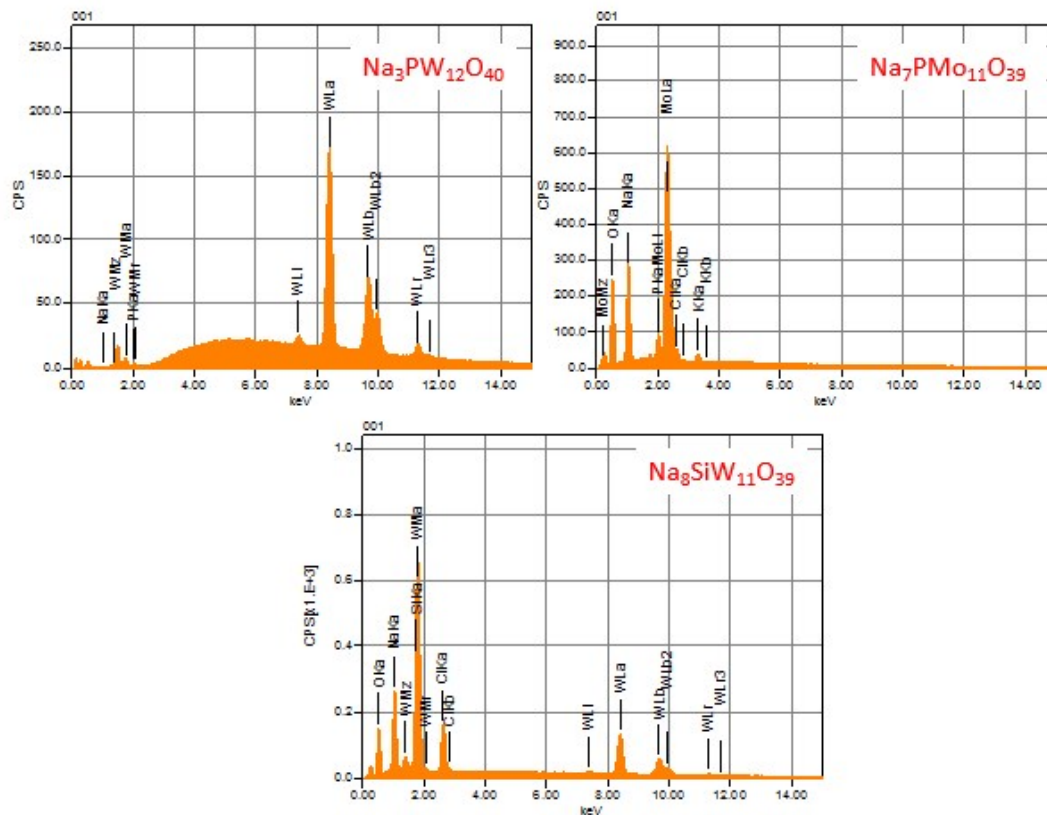


Figure SM10: EDS data of $\text{Na}_3\text{PW}_{12}\text{O}_{40}$, $\text{Na}_7\text{PMo}_{11}\text{O}_{39}$ and $\text{Na}_8\text{SiW}_{11}\text{O}_{39}$

Table SM1. Blank-reactions performed in the absence of the catalyst^a

Exp	Temperature (K)	Conversion (%)	Selectivity (%)			
			Aldehyde	Epoxide	Diepoxide	Alkyl peroxides
1	298	6	0	11	0	91
2	308	7	0	10	0	90
3	318	15	0	11	0	89
4	328	18	0	11	0	89
5	338	24	0	10	0	90

^aReaction conditions: nerol (2.75 mmol); H_2O_2 (5.50 mmol); time (4 h); CH_3CN (10 mL)